PERGAMON

Vision Research 40 (2000) 1785–1795

Vision Research

www.elsevier.com/locate/visres

Electrical multisite stimulation of the isolated chicken retina

Alfred Stett [a,b,*], Wolfgang Barth [a,b], Stefan Weiss [a], Hugo Haemmerle [a], Eberhart Zrenner [b]

[a] *NMI Natural and Medical Sciences Institute, Markwiesenstrasse 55, D-72770 Reutlingen, Germany*
[b] *Department of Experimental Ophthalmology, University Eye Hospital, Roentgenweg 11, D-72076 Tuebingen, Germany*

Received 11 February 1999; received in revised form 5 December 1999

Abstract

Visual prostheses such as subretinal implants are intended for electrical multisite excitation of the retinal network. To investigate relevant issues like spatial resolution and operational range, we have developed an in vitro method using microelectrode arrays to stimulate isolated retinae. Ganglion cell activity in the chicken retina evoked by distally applied spatial voltage patterns consisted of fast bursts, transient inhibition and delayed discharges, and depended on the amount, location and spatial pattern of the injected charge. The response was altered or disappeared when synaptic transmission was blocked. Our results indicate that shape perception and object location can be partially achieved with subretinal electrical multisite stimulation.

Keywords: Visual prosthesis; Microelectrode array; Functional electrical stimulation; Retina preparation; Subretinal stimulation

1. Introduction

Visual prostheses aim at restoring vision to blind humans by multifocal electrostimulation of individual neurons or neural tissue at different locations in the visual pathway. Prostheses are envisioned for stimulating the distal retina with subretinal implants (Chow & Chow, 1997; Zrenner, Miliczek, Gabel, Graf, Guenther, Haemmerle et al., 1997; Peyman, Chow, Liang, Chow, Perlman & Peachey, 1998; Zrenner, Stett, Weiss, Aramant, Guenther, Kohler et al., 1999), the proximal retina with epiretinal implants (Humayun, de Juan, Dagnelie, Greenberg, Propst & Phillips, 1996; Wyatt & Rizzo, 1996; Eckmiller, 1997; Rizzo & Wyatt, 1997) or the visual cortex with intracortical implants (Normann, Maynard, Guillory & Warren, 1996; Schmidt, Bak, Hambrecht, Kufta, O'Rourke & Vallabhanath, 1996). Subretinally implanted prostheses are intended for patients suffering from progressive degeneration of photoreceptors and the underlying retinal structures in the outer plexiform layer. In instance of *retinitis pigmentosa*, the neuronal network in the inner retina is preserved with a relatively intact morphology (Santos, Humayun, de Juan, Greenberg, Marsh, Klock et al., 1997; Zrenner et al., 1997). Thus, it is appropriate for excitation by extrinsically applied electrical current instead of intrinsically delivered photoelectric excitation. This option requires that basic features of images such as points, bars, edges, etc. can be fed into the retinal network by electrical stimulation of individual sites of the distal retina with a set of individual electrodes.

In order to evaluate parameters for subretinal electrical stimulation, we have established a new in vitro method for electrical multisite stimulation of isolated retinae. Here we report on preliminary results related to issues such as spatial resolution and operational range. In our preparation, we attached pieces of the chicken retina with the photoreceptor side facing microelectrode arrays (MEA), and evoked retinal activity by stimulation with different geometrically defined voltage patterns. With this method, we were able to investigate the dependence of the retinal network response on the strength, shape and location of extrinsically injected spatial charge patterns. This arrangement well imitates the in vivo situation of a subretinally implant with embedded stimulation electrodes. The results indicate

* Corresponding author. Tel.: +49-7121-5153070; fax: +49-7121-5153016.
E-mail address: stett@nmi.de (A. Stett)

0042-6989/00/$ - see front matter
PII: S0042-6989(00)00005-5

that it is well suited for a simple in vitro elaboration of main issues arising from functional electrical multisite stimulation of retinae. Some of the results have been presented in abstract form (Stett, Barth, Haemmerle & Zrenner, 1998).

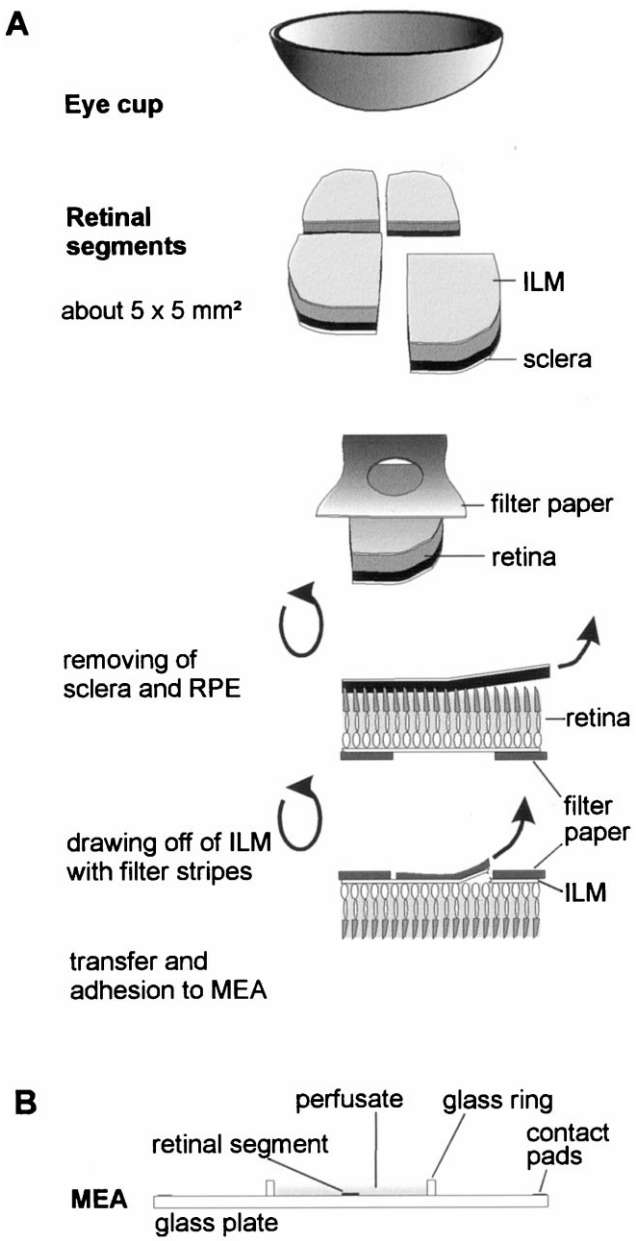

Fig. 1. Preparation of the in vitro retina/MEA (micro electrode array) assemblies. (A) An eyecup is cut into approx. 5×5 mm segments. Sclera, retinal pigment epithelium (RPE) and inner limiting membrane (ILM) are drawn off with tweezers and a piece of filter paper as depicted. Finally, the segment is transferred to the measuring chamber (glass ring) of a MEA. (B) Cross-section of the MEA with adhered retinal segment covering the electrode array (for layout of the array see Fig. 7) which is supported by a glass plate (size 5×5 cm). The electrodes are electrically contacted via the contact pads. The connection lanes between electrodes and contact pads are not shown.

2. Methods

2.1. Retina preparation and perfusate

Newly hatched and dark-adapted chicken (*Gallus domesticus*) were decapitated and the eyes excised. Flat retina pieces were obtained by cutting the eye cup into segments of about 5×5 mm. Pieces of cellulose nitrate filter (Sartorius) with a punched hole at the center were adhered to the ganglion cell side of the segments, which then were rotated to remove sclera and the pigment epithelium (RPE) (Fig. 1A). After an additional rotation, the inner limiting membrane in the center of the retinal segments was drawn off with an additional strip of filter applied for several seconds to the retina. This was to ensure free access to ganglion cell bodies for spike recording with glass pipettes. Finally, retinal segments were attached with the receptor side to the surface of multielectrode arrays (MEA, Fig. 1B). For improving the adhesion, the MEA was initially covered with dissolved cellulose nitrate (1 cm^2 of Sartorius cellulose nitrate filter in 4 ml methanol) dried in air. The preparation was carried out under moderate illumination in standard perfusate (solutes in mM: 100 NaCl, 30 $NaHCO_3$, 50 glucose, 6 KCl, 2 $MgSO_4$, 1 $CaCl_2$, 1 NaH_2PO_4) bubbled with 95% O_2, 5% CO_2 with a pH of 7.5 ± 0.2 and a temperature of 35 ± 1°C. During the experiment the preparation was perfused with the standard solution at a rate of 1 ml/min.

2.2. Multisite stimulation with a microelectrode array (MEA)

The MEA consisted of a 5×5 cm glass plate with 60 substrate integrated and insulated golden connection lanes terminating in an 8×8 array (spacing 100 μm) in the center of the plate (Fig. 1B). Circular openings (diameter 10 μm) in the Si_3N_4 insulation layer at the terminals of the lanes define the size of the stimulation electrodes (Nisch, Böck, Haemmerle & Mohr, 1994). On some MEAs the gold electrodes were covered either with platinum black or a thin titanium nitride (TiN) film to enhance the safe charge injection capability (Janders, Egert, Stelzle & Nisch, 1996).

Each of the 60 MEA electrodes could be individually connected to the output of a computer controlled arbitrary waveform generator (HP33120A, Hewlett-Packard) (Fig. 2A). Monophasic voltage pulses with an amplitude up to 3 V were applied against ground and monitored with a digital multimeter (HP34401A, Hewlett-Packard) and a digital storage oscilloscope (HP54610B, Hewlett-Packard). Pulse duration was usually 0.5 ms. The bath solution was kept at ground potential by an Ag/AgCl pellet. Two-dimensional stimulation patterns at the distal side of the retina such as spots, squares, boxes or bars were obtained by selecting multiple electrodes of the array. The locally injected

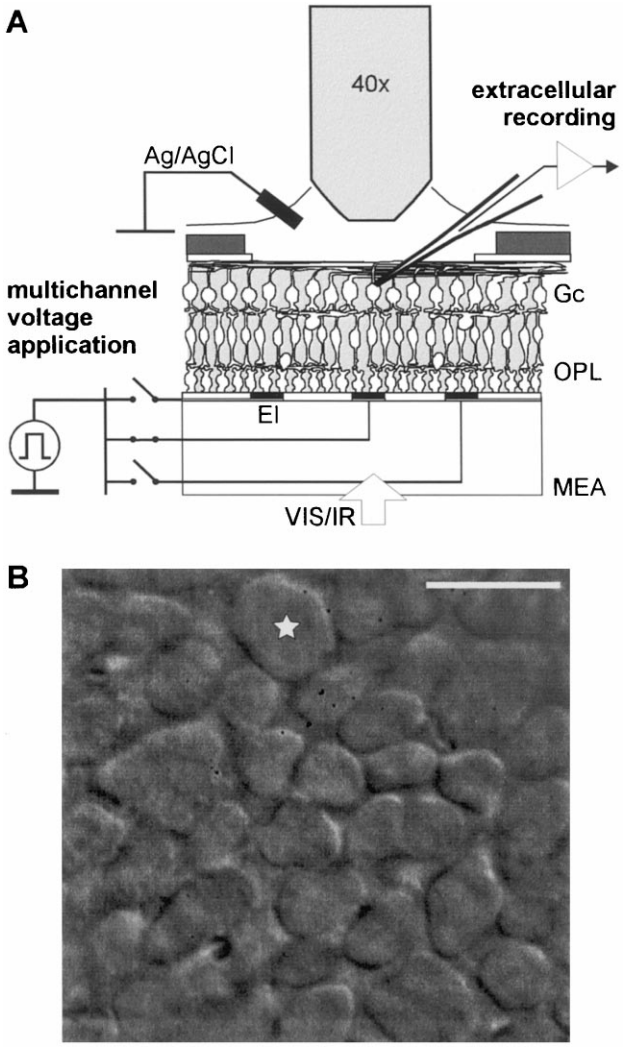

Fig. 2. Setup for distal multisite electrostimulation of retina preparations. (A) Schematic cross-section (unscaled). A retina segment is attached to the surface of a MEA. The preparation is submerged in perfusate and grounded by an Ag/AgCl pellet. The distal retina site faces substrate integrated planar stimulation electrodes (El), which individually can be connected to a voltage pulse generator (left). Spike activity is recorded with a glass electrode from individual ganglion cell bodies (MEA, microelectrode array; Gc, ganglion cell; OPL, outer plexiform layer). (B) Infrared image of cell bodies in the ganglion cell layer. The asterisk indicates a candidate for recording. Scale bar 10 μm.

charge per pulse and electrode was estimated with the retinal segment still adhering to the MEA by measuring the current flow through the reference electrode to ground and subsequent off-line integration of the current transient as explained in Fig. 3.

2.3. Spike recording

Evoked activity was recorded from individual ganglion cell bodies with a glass electrode (opening 1.5 μm, 3 MΩ, filled with bath solution, Fig. 2A) in the loose-patch configuration (Sakmann & Neher, 1983). Experiments were carried out under visual observation with infrared sensitive optics (Zeiss Axiovert; Olympics water-immersion objective 40 × /0.8, IR camera C2440, Hamamatsu; 755 nm band pass filter, monitor) of an Infrared-Patch-Clamp-Setup (Luigs & Neumann). The largest cell bodies (Fig. 2B) were chosen for data collection.

The signal of the glass electrode was recorded with a patch clamp amplifier (0–8 kHz; 10 × ; SEC-05L, npi electronic) in the bridge mode, simultaneously postamplified and filtered with an AC amplifier (0.3–2 kHz, 100 × ; AMS 1800). Analog traces could be observed with a digital storage oscilloscope (HP54610B, Hewlett-Packard) and were sampled (10 kHz, 16 bit) with a software controlled (TIDA 3.0; HEKA elektronik) interface board with analog to digital converters (ITC 16, Instrutech).

2.4. Control experiments

Light sensitivity of the retinal segments was tested in some cases by flashing the microscope light with an electromagnetic shutter. After contacting a cell body with the glass electrode, 50 light pulses of 500 ms duration were presented consecutively with an interstimulus interval of 1500 ms. To ensure that the gan-

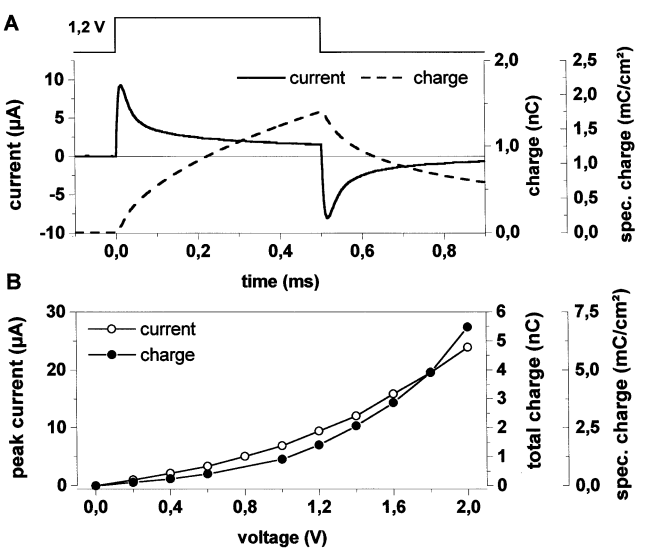

Fig. 3. Electrical stimulation with voltage pulses and estimation of injected charge. (A) The current resulting from a voltage pulse (top trace) applied to a single electrode (platinized gold, ∅ 10 μm) is measured (left scaling) with a current-to-voltage converter connected between ground and Ag/AgCl pellet (cf. Fig. 2). By integration of the current trace, the injected charge is estimated and standardized to the electrode area (broken line, right scaling). The maximum amount of injected charge is reached at the end of the on-phase of the pulse. (B) Peak current and maximum charge per pulse plotted against the applied voltage reveals a non-linear relationship due to the metal–electrolyte interface that acts as a non-ideal, leaky capacitor.

glion cell activity was driven by the network, the original perfusate was replaced by one with increased [Mg^{2+}] and decreased [Ca^{2+}] (in mM: 6 Mg^{2+}, 0.5 Ca^{2+}) to block synaptic transmission or by one with selective agents like 2-amino-4-phosphono-butyric acid (APB, AP4) or kynurenic acid (both 100 μM) (Slaughter & Miller, 1981; Fujimoto & Toyoda, 1991; Wu, 1994).

2.5. Electrical stimulation protocol and data analysis

The extracellular stimulation procedures began after formation of a stable contact of the glass electrode to a cell body and some light stimulation trials were achieved. The experiment was conducted by increasing the number of electrodes surrounding the recording site and increasing the voltage amplitude successively until a clear stimulus-correlated spike activity was observed. The subsequent recordings contained up to 50 trials with an interstimulus interval of 1500 ms. Stored data were processed off-line by a spike extraction program using a threshold algorithm. From these data, rasterplots and peristimulus time histograms (PSTH) of the responses were obtained.

3. Results

3.1. Electrical evoked spike activity of individual ganglion cells

We recorded stimulus-correlated activity from 48 ganglion cells from 28 retinae. Electrical stimulation of the retinal segments with short voltage pulses resulted in typical temporal spike patterns of ganglion cells. Examples of analog traces, rasterplots and response histograms obtained from representative cells are shown in Fig. 4. Temporal spike patterns consisted of a single burst with latencies of about 10–20 ms (Fig. 4A), a weak delayed discharge (Fig. 4B) or a vigorous, early burst followed by a silent period and a delayed discharge with smaller amplitude (Fig. 4C). Shortest latencies of the first spikes in the early burst were down to 1 ms (Fig. 4C). In no case was an unambiguous response to light stimulus observed.

3.2. Charge dependency of the response

The response of the ganglion cells depended on the amplitude of the applied voltage pulse as shown in Fig.

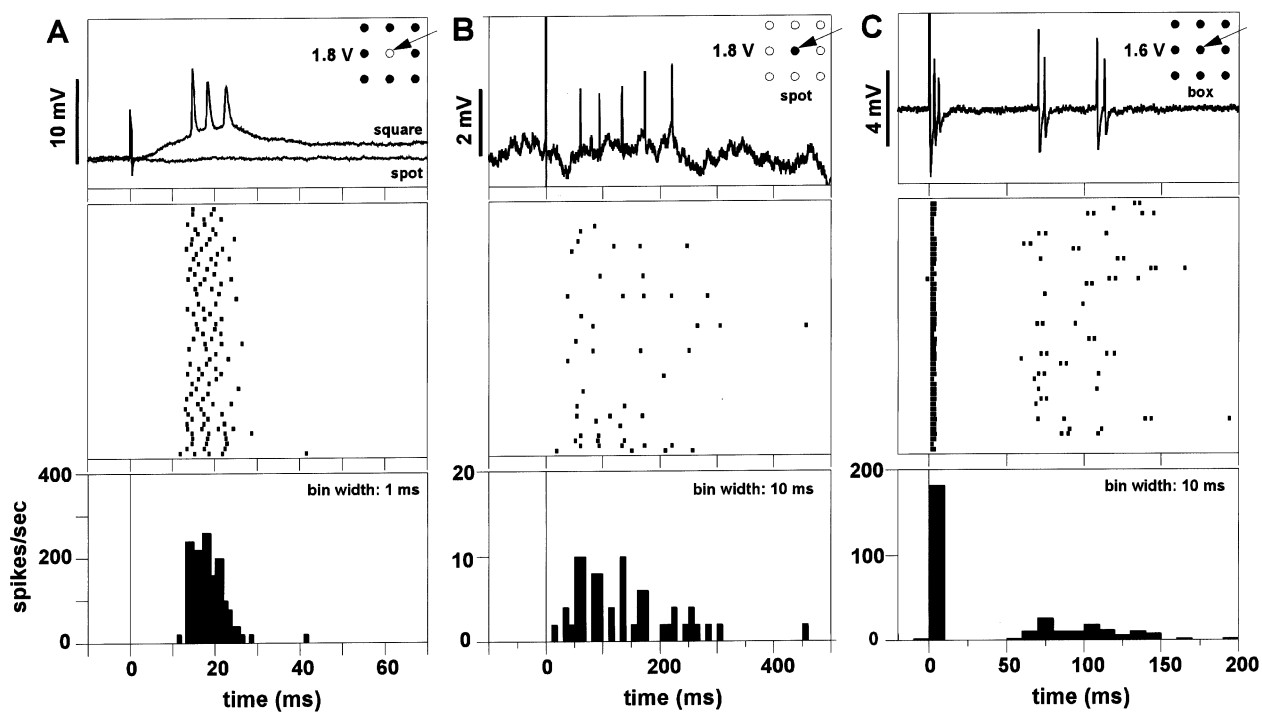

Fig. 4. Responses of different ganglion cells evoked by single voltage pulses (amplitudes as indicated, pulse duration 0.5 ms). Analog traces from extracellular loose-patch recordings, rasterplots and peristimulus time histograms (PSTH) of 50 trials (from top to bottom). Voltage has been applied to gold electrodes underneath and surrounding the recording site at time $t = 0$ (filled circles in sketches in upper plots, arrowhead: recording site). (A) Response consisting of a single burst with a latency of about 13 ms. No response occurred with the spot-like stimulation pattern. (B) Weak, delayed discharges with latencies of about 50 ms. (C) Spike response pattern consisting of a vigorous short latency peak, followed by a transient inhibition and a delayed discharge.

5(A) for three selections of stimulation electrodes. The rasterplots and PSTHs in the left column are obtained from spot-like stimulation with a single electrode underneath the recording side as depicted in the sketch above. A voltage threshold of about 0.6 V had to be surpassed in order to elicit a reliable response in all subsequent trials. The higher the voltage level, the more precise was the strength and the timing of the response: after a short latency, the pulse was followed by a single burst; the number of the spikes within this burst increased with increasing voltage level while the latency was shortened (compare responses with the 1.2 and 1.8 V pulses). The reliability of the response to a certain voltage level is demonstrated by cumulative histograms, where the maximum number of spikes within a 1-ms bin is almost equal to the number of subsequent trials. A similar behavior could be observed for the other spatial voltage patterns, i.e. the square (Fig. 5A, middle column) and the box (Fig. 5A, right column).

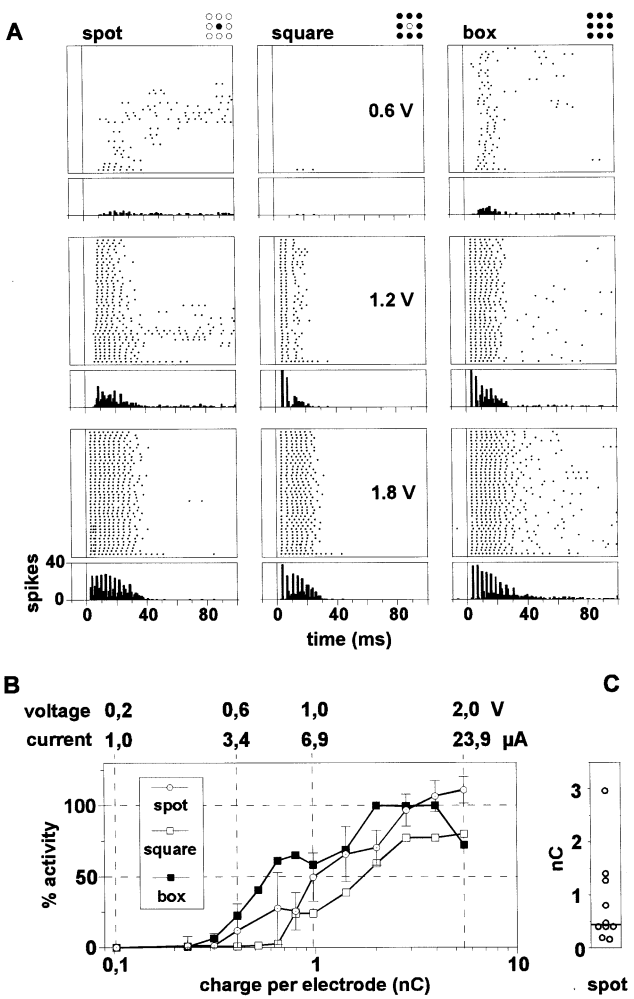

Fig. 5. Evoked response related to strength and pattern of injected charge. (A) Raster plots (40 trials) and cumulative response histograms (bin width 1 ms) to a single voltage pulse with 0.5 ms duration and increasing amplitude, applied to a spot- (left column), a square- (middle column) or a box- (right column) like selection of platinized gold electrodes. In the histograms the number of spikes from 40 trials is given. (B) Relative ganglion cell response in a 40 ms window after pulse onset plotted against charge injected per pulse and electrode. At the upper x-axis the related voltage level and peak current are given (cf. Fig. 3). The response has been standardized to the maximum spike number obtained with box stimulation. Error bars are given for the spot data curve. They indicate the standard deviation of the number of spikes per trial within the analyzing window. (C) Scatter diagram showing the charge thresholds for spot stimulation ($n = 10$). The line represents the median value (0.43 nC).

To quantify the dependence of the response on the voltage level and spatial pattern, we analyzed the spike rate in a response window (40 ms) after the onset of the pulse and constructed tuning curves of relative spike activity as shown in Fig. 5(B). The evoked activity was standardized to the maximum of the response to the box-like stimulation pattern and plotted against the logarithm of the charge injected per electrode and pulse (see Fig. 3 for charge estimation procedure). In the given example, the tuning curves for the spot and box pattern gave the same threshold of about 0.4 nC per electrode (500 µC/cm^2, obtained from the next data point above the 10% level of the respective curve). The threshold for square stimulation was about 0.7 nC per electrode (875 µC/cm^2). Fig. 5(C) shows the distribution of the charge thresholds for spot stimulation with a median value of 0.4 nC ($n = 10$). No significant differences were found so far for box and square stimulation.

A common feature of the curves is the steep slope interrupted by two steps at about 0.6–0.8 nC and 1.1–1.2 nC. The upper limits of the curves are determined by the charge injection limit of the electrodes of about 2 V. Therefore, it can not be decided if the curves reached a saturation level with decreasing spike rates as indicated by the box tuning curve or if there are further steps of activity.

3.3. Proof of network stimulation

One of the goals of our experiments was to show that the retinal network is stimulated by distal charge injection prior to ganglion cell activity. On the assumption that spike activity locked to consecutive stimulation results from synaptically transmitted network activity, we applied in control experiments ($n = 11$) a perfusate with higher Mg^{2+} concentration (6 mM) to block all synaptic transmissions. As expected, under this condition in most of our control experiments all activity evoked with certain patterns disappeared completely ($n = 6$), as shown in Fig. 6 (second row). In general, the response recovered after removal of high Mg^{2+} concentration (Fig. 6, third row). With this perfusate, all features of the response obtained under normal conditions with spot and square stimulation were extinguished. However, the fast spike and the delayed

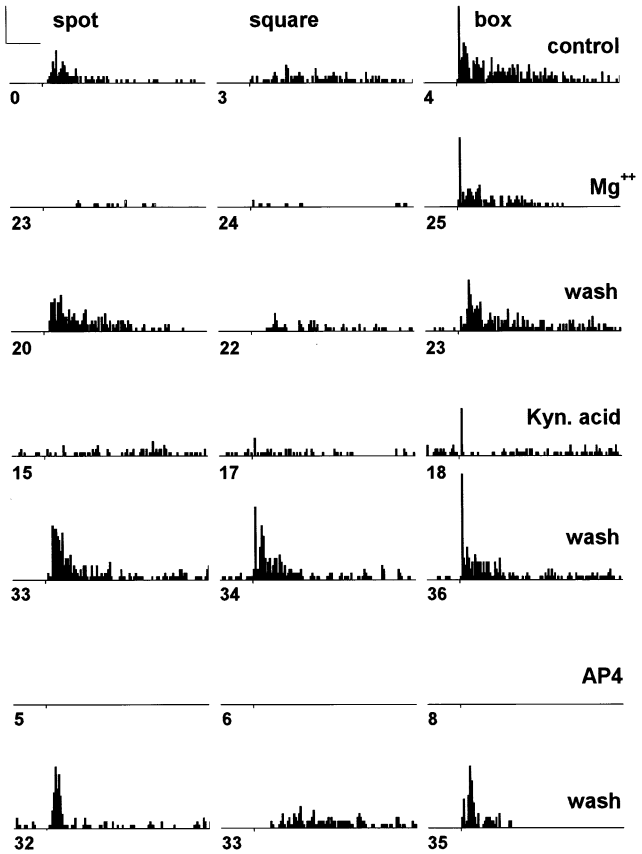

Fig. 6. Effect of high [Mg^{2+}], Kynurenic acid and AP4 to the spike activity evoked by single voltage pulses (2 V, 0.5 ms, applied at time indicated by the short tick on x-axis; TiN electrodes). Response histograms with binwidth 5 ms from 20 repetitions. The number at each histogram indicates the time interval (minutes) after switching to the perfusate with the agents given at the right and to the standard perfusate for washing out the agents, respectively. Scale bars 100 ms, 100 spikes/s (top lefthand corner).

response evoked by box stimulation were only reduced. In some experiments ($n = 3$) the delayed response components disappeared totally while the fast spikes remained, or the effect was not clear ($n = 2$).

For a more selective effect on synaptic transmissions in the outer retina, we also tested perfusates containing 100 μM AP4 ($n = 10$) or kynurenic acid ($n = 5$). In the example shown in Fig. 6 (fourth row), the glutamate antagonist kynurenic acid suppressed all responses except the fast spike evoked by the box-like pattern. It also caused an increased spontaneous activity and an increased excitability after switching back to the standard perfusate (fifth row). The glutamate agonist AP4 totally extinguished the increased spontaneous activity caused by kynurenic acid and also suppressed all stimulus-correlated response Fig. 6 (sixth row). The recovery after serial application of the agents was not complete (lower row). This might be due to an incomplete wash out of the substances or to the long time interval of about 3 h needed to complete the experiment.

In experiments, where the response of the ganglion cells failed to appear by adding the agents to the perfusate ($n = 6$ with Mg^{2+}, $n = 5$ with AP4, $n = 3$ with kynurenic acid), we could confidentially exclude that the evoked spike patterns were caused by direct ganglion cell stimulation. Other results, where the response was distinctly altered but not totally suppressed ($n = 5$ with Mg^{2+}, $n = 2$ with AP4; $n = 2$ with kynurenic acid), supported an action presynaptic to ganglion cells mediating the specific response of the retinal network.

3.4. Pattern dependence

We considered whether the distinguishable responses to different patterns were caused by the shape and location of the pattern or by the number of selected electrodes. In the example shown in Fig. 5, the activity evoked by the single electrode beneath the recorded ganglion cell is lower than the one evoked by the box (nine electrodes), but larger than the one evoked by the square (eight electrodes), over almost the entire operational range. At a high voltage level, the ganglion cells firing rate evoked by the box even becomes lower than the one evoked by the other patterns. In the example shown in Fig. 6 (first row), the spot stimuli caused a transient discharge with a latency of 40 ms (median value of the first spike after pulse onset in 20 trials), whereas the square pattern evoked a weak and blurred response with a latency of 110 ms. The box-like pattern evoked an early burst response with a latency of 5 ms, followed by a vigorous transient discharge

From this results, we concluded that the evoked activity pattern does not only depend on the number of electrodes within a certain area containing the recording site. It also depends on the distribution of the selected electrodes within that area.

3.5. Distance related activity

The spatial resolution of local electrical stimulation is related to the spatial extent of the elicited retinal response. To test the spatial sensitivity, we produced a bar-like spatial stimulation pattern by selecting a row or a column of electrodes (Fig. 7). The response of the ganglion cell was dependent both on the distance of the bar to the recording site and the applied voltage level, as shown in Fig. 7(A). With a 0.8 V pulse the spike rate was transiently increased only when the bar crossed the recording site, whereas with 1.2 and 1.6 V pulses the ganglion cell responded with a single burst also at a distance of 100 μm from the recording site. In the given example, the response was not symmetrical around the recording site. The bar 100 μm distant from the recording site evoked the maximum spike rate, whereas at −100 μm no burst was evoked. This may be because the recording site was displaced somewhat from the

central electrode. In no case was an increased spike rate observed at distances larger than 200 μm ($n = 4$). We include the result in the tuning curves depicted in Fig. 7(B). The response measure in the upper plot was the difference between the number of spikes within a 40 ms analyzing window following the pulse onset and the spontaneous activity level before pulse onset. Both the maximum spike number and the width of the curves increased with increasing voltage level.

We also analyzed the overall temporal response to repetitive stimulation. The response measure in the lower plot of Fig. 7(B) is the difference between the number of spikes within a 200 ms analyzing window after pulse onset and the spontaneous activity. The curves exhibit a distinct shape with a maximum activity around the recording site independent from the direction of the bar. Stimulation of the surrounding region at a distance of about 100–200 μm from the recording

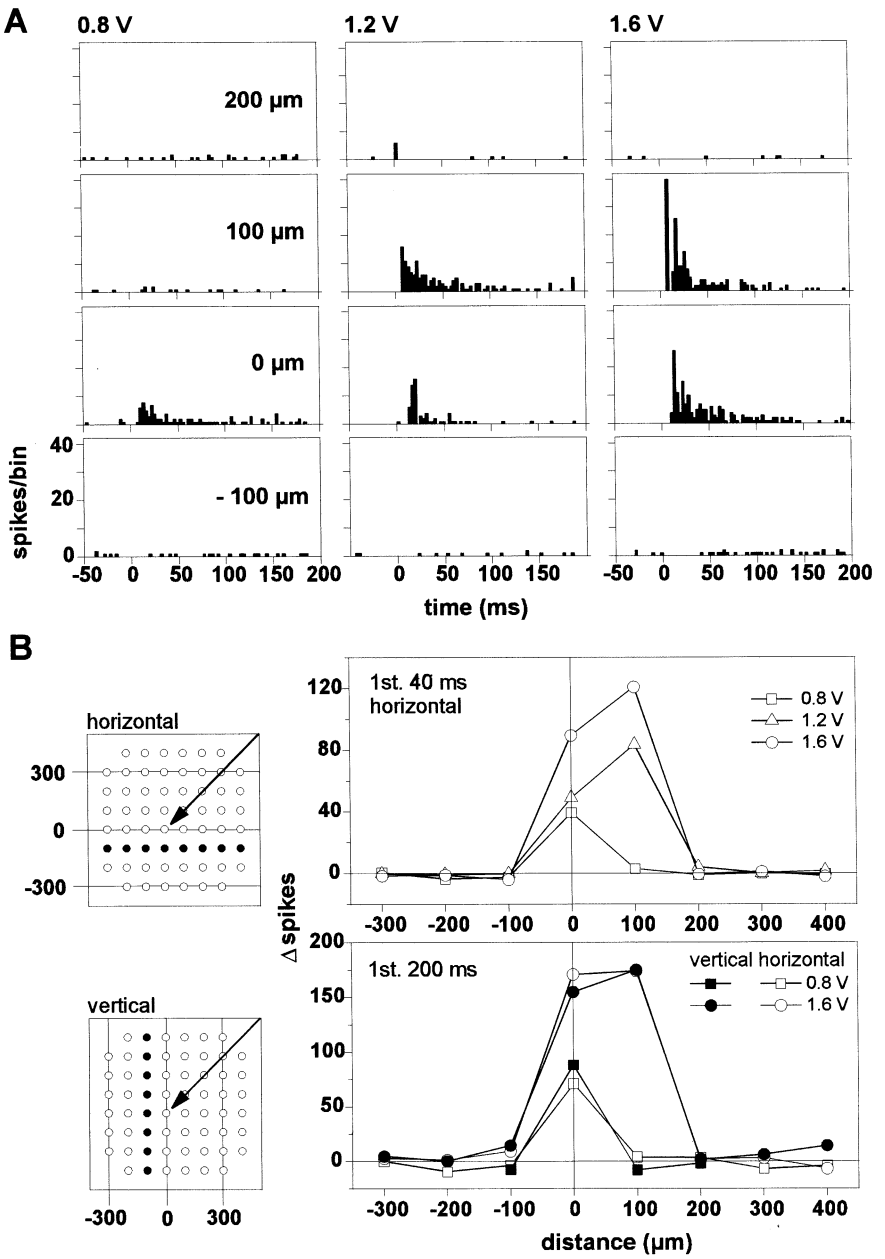

Fig. 7. The dependence of the evoked response on the distance of a charge injection bar. (A) Cumulative response histograms (40 trials, bin width 3 ms) evoked by a single voltage pulse of varying amplitude (columns: 0.8, 1.2, 1.6 V; duration 0.5 ms) applied to a bar-like selection of platinized gold electrodes at different distances from the recording site (rows: −100, 0, 100, 200 μm). (B) Activity depending upon strength, distance and orientation of a bar. The maps at the left indicate the orientation and distance convention of the bar (distances in μm) and the recording site (arrowhead). The tuning curves represent the alteration of the spike activity within the first 40 ms after pulse onset for different pulse amplitudes (top, horizontal bar) and within the first 200 ms after pulse onset for different orientations and pulse amplitudes (bottom, 0.8 and 1.6 V, horizontal and vertical bar). Data points were obtained by subtracting the mean number of spikes in a corresponding window before the pulse onset.

site with low voltage amplitude resulted in a slight reduction of the spike activity below the spontaneous level. This effect was not observable with high voltage levels. Moreover, repetitive stimulation of the center at high amplitudes constrains all activity into a discrete time window following the brief stimulation pulse.

4. Discussion

4.1. Transretinal network excitation

Several in vitro experiments with isolated retinae from carp (Byzov & Trifonov, 1968; Kaneko & Saito, 1983; Toyoda & Fujimoto, 1984; Takahashi & Murakami, 1988) and frog (Knighton, 1975) have shown that neuronal activity can be evoked and modulated by polarizing photoreceptors and retinal interneurones, thereby influencing the synaptic interactions with homogeneous transretinal applied currents. In addition, acute in vivo experiments with cat (Granit, 1946; Gernandt and Granit, 1947), rabbit (Crapper & Noell, 1963; Lederman & Noell, 1969; Molotchnikoff, 1976) and monkey (Ogden & Brown, 1964) have revealed that transretinal current stimulation of intact retinae leads to typical patterns of ganglion cell activity. Local electrical surface stimulation of the inner retina in eyes of rabbits with induced outer retinal degeneration elicited restricted retinal responses (Humayun, Propst, de Juan, McCormick & Hickingbotham, 1994). Electrical evoked cortical potentials could also be recorded after electrical stimulation with chronically implanted electrodes in the epiretinal space of cats (Dawson & Radtke, 1977) and subretinal space of rabbits (Chow & Chow, 1997).

Although these results are intriguing and reveal the basic effects of electrical retina stimulation, very little is yet known concerning the spatial resolution and operational range for network activation arising from patterned stimulation. To explore these basic issues of functional electrical multisite stimulation of retinae, we have developed a new in vitro method using a microelectrode array (MEA) similar to that used by others for multichannel recording of retinal activity (Haemmerle, Egert, Mohr & Nisch, 1994; Meister, Pine & Baylor, 1994). Arrays of planar stimulation sites are a well suited in vitro multichannel stimulation tool for variable multisite stimulation of single cells (Stett, Müller & Fromherz, 1997) or tissue preparations (Borkholder, Bao, Maluf, Perl & Kovacs, 1997).

For evaluating our methods we used segments of isolated chicken retina, because the preparation of the retina is relatively simple. We are aware of the fact that there are differences between the organization of the avian retina and the retina of higher mammals (Holden, 1982). However, we think that these differences can be neglected if one wants to study the basic parameters that are important for functional electrical stimulation of isolated retinae.

Ganglion cells from which recordings were taken were selected according to a size criterion. They were larger than displaced amacrine cells which migrated to the ganglion cell layer (Ehrlich, 1981). We were able to elicit typical ganglion cell spike patterns that depended on the spatial pattern, strength and location of distally applied, brief voltage pulses. In control experiments, the stimulus-correlated spike activity disappeared after adding high [Mg^{2+}] to the perfusate. We attribute this result to blocked synaptic transmission by increased [Mg^{2+}] and could exclude direct ganglion cell stimulation in these cases. Thus, we were able to locate the stimulated structure within the retinal network. This interpretation is additionally supported by the distinct effects on the evoked activity of the glutamate agonist AP4, which selectively blocks the synaptic transmission of photoreceptors to bipolar cells in the on-pathway (Slaughter & Miller, 1981; Wu, 1994), and kynurenic acid which selectively suppresses the off-pathway at the level of receptor-bipolar synapse (Fujimoto & Toyoda, 1991). In the cases where the response of the ganglion cells to the electrical stimuli is blocked by these agents, it can be therefore concluded, that the distally applied electrical stimulus primary stimulates the receptors.

However, in some cases the spikes that immediately followed the stimulus (Figs. 4 and 6) did not disappear at high stimulation strength after adding high [Mg^{2+}] to the perfusate. We attribute this behavior to direct stimulation of ganglion cell bodies or axons, in agreement with the interpretation of Crapper and Noell (1963). Their study dealt with the rabbit retina. It was concerned with the effects of transretinal current pulse stimulation measured by the discharge activity of the ganglion cells. They concluded that the proximal part of the photoreceptors is the primary target of the electrical stimulus, and that the inhibitory phenomena are primarily induced within the outer plexiform layer. Transretinal stimulation additionally affects the inner plexiform layer in the same manner. This influence, which is essential for electrical stimulation of retinas with a degenerated outer plexiform layer by a subretinal implant, may be separated with specific pharmacological agents.

4.2. Operational range

Our decision to use voltage pulses instead of the more commonly used current pulses was dictated by the need to obtain an easier control over electrode polarization during the multielectrode stimulation. Application of voltage to the electrodes charges the capacity of the

electrical double layer of the metal–electrolyte interface. This leads to fast, strong but transient capacitive currents with opposite sign at the rising and falling edges of voltage pulses (cf. Fig. 2B), resulting in transient hyperpolarization and depolarization of cellular membranes (Fromherz & Stett, 1995). This is similar to the effect of brief biphasic current pulses commonly used for safe tissue stimulation (Tehovnik, 1996). In both cases, however, membrane polarization of the target neurons is primary affected by the voltage gradient generated by the local current density and tissue resistance in the vicinity of the cells and therefore depends on the effective spread of the injected current within the electrode–tissue interface and within the tissue.

It is customary to express the stimulation strength in charge injected per pulse, often standardized to the geometric area of the stimulation electrode. The charge injected with current pulses depends only on the amplitude and duration of the pulse whereas with controlled voltage pulses the charge additionally depends on the tissue resistance and the capacity of the electrode–tissue interface. To minimize the influence of alterations of these parameters on the charge tuning curves (Fig. 5) we therefore estimated the charge per voltage pulse by measuring the resulting current with the retinal segment still adhering to the MEA surface. The median value of the charge needed with a single electrode (geometric area about 80 μm^2) to reach threshold was 0.4 nC. This threshold charge is lower than those reported so far for focal retina stimulation. For example, Humayun et al. (1994) reported a threshold charge of 3.75 nC for bipolar surface stimulation (geometric electrode area: 12 600 μm^2) of bullfrog eyecups with biphasic square current pulses of 75 μs duration per half phase. Our lower values might be due to a very close contact between the flat mounted retina segment and the planar electrodes obtained by sticking the retina with the cellulose nitrate to the MEA surface.

The course of the charge tuning curves in Fig. 5 reveals a threshold phenomenon for electrical retina excitation. They also span the margin for distal retina stimulation. The neuronal thresholds give the lower limit, whereas the safe charge injection limit of the electrodes gives the upper limit. The resulting operational range for modulating the spike activity with distally injected charge covers about one and half orders of magnitude. If one replaces charge by luminance as the means of stimulation, the shape and extent of the tuning curves is almost the same as obtained by stimulation of the intact retina with light spots flashed on a background at constant background illuminance (Sakmann & Creutzfeldt, 1969).

4.3. Spatial sensitivity

The spatial influence of an electrical stimulus locally applied with a single electrode is a crucial issue when considering the spatial resolution attainable by functional retina stimulation. Increasing the amplitude of voltage pulses not only increases the local impact but also leads to marked cell polarization of an increasing vicinity around the stimulating electrode. Therefore, it may assumed that the spatial resolution decreases with increasing stimulation strength. This means that the half width of the distance tuning curves in Fig. 7(B) should become broader with an increasing voltage level. The spacing of 100 μm of the MEA electrodes, however, prevents a more detailed examination of this issue. Despite this limitation, the plots clearly reveal that the sensitivity of ganglion cells to locally applied charge injection patterns is spatially confined up to distances of some hundred microns. It remains to be shown wether the distance tuning curves obtained from the bar-like electrical stimulations can be described by a formula similar to the line width function of light receptive fields with an excitatory center and an inhibitory surround area (Rodieck, 1965; Wandell, 1995). If the shape of the distance-tuning curve is due to electrically evoked lateral interactions within the area of the receptive field of the ganglion cell, then adding GABA to the perfusate should influence it. GABA is a known specific inhibitory transmitter acting in lateral retinal pathways and subserving the center-surround characteristic of receptive fields (Barnstable, 1993). Such issues are the object of further experiments in which we will also attempt to fit the curves with Gaussian like functions.

Our results from chicken retina indicate that basic features of images can be transformed into activity of intact retinal network by excitation of receptive field morphology through distally applied spatial voltage patterns. First results obtained from rat retina in which the photoreceptors and outer plexiform layer have degenerated show that such artificial stimuli can also lead to discriminating network activity (Zrenner et al., 1999). From the viewpoint of functional electrical stimulation, it is likely that shape perception and object location will be possible with subretinal electrical multisite stimulation. Hence, the subretinal approach is a promising alternative for providing a retinal prosthesis.

Acknowledgements

This work is supported by the BMBF Grants 01IN502 A,C; fortüne Grant Nr. 233, University of Tuebingen; and in part by a donation from Hewlett Packard GmbH, Boeblingen, Germany. The MEAs were manufactured at the Dept. of Applied Physics (Head: Dr Wilfried Nisch) at the Natural & Medical Sciences Institute (NMI) in Reutlingen. We thank Andreas Mai for contributing experimental results, Prof. Lindsay T. Sharpe and Dr Michael Fejtl for reading the manuscript.

References

Barnstable, C. J. (1993). Glutamate and GABA in retinal circuitry. *Current Opinion in Neurobiology*, *3*, 520–525.

Borkholder, D. A., Bao, J., Maluf, N. I., Perl, E. R., & Kovacs, G. T. A. (1997). Microelectrode arrays for stimulation of neural slice preparations. *Journal of Neuroscience Methods*, *77*, 61–66.

Byzov, A. L., & Trifonov, J. A. (1968). The response to electric stimulation of horizontal cells in the carp retina. *Vision Research*, *8*, 817–822.

Chow, A. Y., & Chow, V. Y. (1997). Subretinal electrical stimulation of the rabbit retina. *Neuroscience Letters*, *225*, 13–16.

Crapper, D. R., & Noell, W. K. (1963). Retinal excitation and inhibition from direct electrical stimulation. *Journal of Neurophysiology*, *26*, 924–947.

Dawson, W. W., & Radtke, N. D. (1977). The electrical stimulation of the retina by indwelling electrodes. *Investigative Ophthalmology & Visual Science*, *16*, 249–252.

Eckmiller, R. (1997). Learning retina implants with epiretinal contacts. *Ophthalmic Research*, *29*, 281–289.

Ehrlich, D. (1981). Regional specialization of the chick retina as revealed by the size and density of neurons in the ganglion cell layer. *The Journal of Comparative Neurology*, *195*, 643–657.

Fromherz, P., & Stett, A. (1995). Silicon-neuron junction: capacitive stimulation of an individual neuron on a silicon chip. *Physical Review Letters*, *75*, 1670–1673.

Fujimoto, M., & Toyoda, J. (1991). An analysis of inputs to ON–OFF amacrine cells in the carp retina with kynurenic acid. *Neuroreport*, *2*, 317–320.

Gernandt, B., & Granit, R. (1947). Single fiber analysis of inhibition and the polarity of the retinal elements. *Journal of Neurophysiology*, *10*, 295–301.

Granit, R. (1946). The distribution of excitation and inhibition in single-fiber responses from a polarized retina. *Journal of Physiology*, *105*, 45–53.

Haemmerle, H., Egert, U., Mohr, A., & Nisch, W. (1994). Extracellular recording in neuronal networks with substrate integrated microelectrode arrays. *Biosensors & Bioelectronics*, *9*, 691–696.

Holden, A. L. (1982). Electrophysiology of the avian retina. In N. Osborne, & G. Chader, *Progress in retinal research*. Oxford: Pergamon Press.

Humayun, M., Propst, R., de Juan, E. Jr, McCormick, K., & Hickingbotham, D. (1994). Bipolar surface electrical stimulation of the vertebrate retina. *Archives of Ophthalmology*, *112*, 110–116.

Humayun, M. S., de Juan, E. Jr, Dagnelie, G., Greenberg, R. J., Propst, R. H., & Phillips, D. H. (1996). Visual perception elicited by electrical stimulation of retina in blind humans. *Archives of Ophthalmology*, *114*, 40–46.

Janders, M., Egert, U., Stelzle, M., Nisch, W. (1996). Novel thin film micro-electrodes with excellent charge transfer capability for cell stimulation and sensing applications. *Proceedings of the 18th Annual International Conference of the IEEE Engineering in Medicine and Biology Society*, # 364.

Kaneko, A., & Saito, T. (1983). Ionic mechanisms underlying the responses of off-center bipolar cells in the carp retina. II. Studies on responses evoked by transretinal current stimulation. *The Journal of General Physiology*, *81*, 603–612.

Knighton, R. W. (1975). An electrically evoked slow potential of the frog's retina. I. Properties of response. *Journal of Neurophysiology*, *38*, 185–197.

Lederman, R. J., & Noell, W. K. (1969). Optic nerve population responses to transretinal electrical stimulation. *Vision Research*, *9*, 1041–1052.

Meister, M., Pine, J., & Baylor, D. A. (1994). Multi-neuronal signals from the retina: aquisition and analysis. *Journal of Neuroscience Methods*, *51*, 95–106.

Molotchnikoff, S. (1976). Transient response of rabbit retinal ganglion cells to photic and electrical stimuli. *Canadian Journal of Neurological Sciences*, *3*, 73–79.

Nisch, W., Böck, J., Haemmerle, H., & Mohr, A. (1994). A thin film microelectrode array for monitoring extracellular neuronal activity in vitro. *Biosensors & Bioelectronics*, *9*, 737–741.

Normann, R. A., Maynard, E. M., Guillory, K. S., & Warren, D. J. (1996). Cortical implants for the blind. *IEEE Spectrum*, *33*, 54–59.

Ogden, T. E., & Brown, K. T. (1964). Intraretinal responses of the cynamolgus monkey to electrical stimulation of the optic nerve and retina. *Journal of Neurophysiology*, *27*, 682–705.

Peyman, G., Chow, A. Y., Liang, C., Chow, V. Y., Perlman, J. I., & Peachey, N. S. (1998). Subretinal semiconductor microphotodiode array. *Ophthalmic Surgery and Lasers*, *29*, 234–241.

Rizzo, J. F., & Wyatt, J. (1997). Prospects for a visual prosthesis. *The Neuroscientist*, *3*, 251–262.

Rodieck, R. W. (1965). Quantitative analysis of cat retinal ganglion cell response to visual stimuli. *Vision Research*, *5*, 583–601.

Sakmann, B., & Creutzfeldt, O. D. (1969). Scotopic and mesopic light adaption in the cat's retina. *Pflügers Archives*, *313*, 168–185.

Sakmann, B., & Neher, E. (1983). *Single-channel recording*. New York and London: Plenum Press.

Santos, A., Humayun, M. S., de Juan, E. Jr, Greenberg, R. J., Marsh, M. J., Klock, I. B., & Milam, A. H. (1997). Preservation of the inner retina in retinitis pigmentosa. A morphometric analysis. *Archives of Ophthalmology*, *115*, 511–515.

Schmidt, E. M., Bak, M., Hambrecht, F. T., Kufta, C. V., O'Rourke, D. K., & Vallabhanath, P. (1996). Feasibility of a visual prosthesis for the blind based on intracortical microstimulation of the visual cortex. *Brain*, *119*, 507–522.

Slaughter, M. M., & Miller, R. F. (1981). 2-Amino-4-phosphonobutric acid: a new pharmacological tool for retina research. *Science*, *211*, 182–185.

Stett, A., Müller, B., & Fromherz, P. (1997). Two-way silicon–neuron interface by electrical induction. *Physical Review E*, *55*, 1779–1782.

Stett, A., Barth, W., Haemmerle, H., & Zrenner, E. (1998). Network activity of the chicken retina electrically evoked by distally applied spatial voltage patterns. *Proceedings of the 26th Goettingen Neurobiology Conference*, *Vol. II* (437). Stuttgart, New York: Thieme.

Takahashi, K., & Murakami, M. (1988). Calcium action potential in on–off transient amacrine cell of the carp retina. *Brain Research*, *456*, 29–37.

Tehovnik, E. J. (1996). Electrical stimulation of neural tissue to evoke behavioral responses (review article). *Journal of Neuroscience Methods*, *65*, 1–17.

Toyoda, J., & Fujimoto, M. (1984). Application of transretinal current stimulation for the study of bipolar-amacrine transmission. *The Journal of General Physiology*, *84*, 915–925.

Wandell, B. A. (1995). *Foundations of vision*. Sunderland, MA: Sinauer Associates, Inc.

Wu, S. M. (1994). Synaptic transmission in the outer retina. *Annual Review of Physiology*, *54*, 141–168.

Wyatt, J., & Rizzo, J. (1996). Ocular implants for the blind. *IEEE Spectrum*, *33*, 47–53.

Zrenner, E., Miliczek, K. D., Gabel, V. P., Graf, H. G., Guenther, E., Haemmerle, H., Hoefflinger, B., Kohler, K., Nisch, W., Schubert, M., Stett, A., & Weiss, S. (1997). The development of subretinal microphotodiodes for replacement of degenerated photoreceptors. *Ophthalmic Research*, *29*, 269–280.

Zrenner, E., Stett, A., Weiss, S., Aramant, R. B., Guenther, E., Kohler, K., Miliczek, K. D., Seiler, M. J., & Haemmerle, H. (1999). Can subretinal microphotodiodes successfully replace degenerated photoreceptors? *Vision Research*, *39*, 2555–2567.